Prognostic and Warning System for Power-Electronic Modules in Electric, Hybrid Electric, and Fuel-Cell Vehicles

Yali Xiong, *Student Member, IEEE*, Xu Cheng, *Member, IEEE*, Z. John Shen, *Senior Member, IEEE*, Chunting Mi, *Senior Member, IEEE*, Hongjie Wu, and Vijay K. Garg, *Fellow, IEEE*

Abstract—Reliability of power-electronic modules is of paramount importance for the commercial success of various types of electric vehicles. In this paper, we study the technical feasibility of detecting and utilizing early symptoms and warning signs of power-module degradation due to thermomechanical stress and fatigue and develop a prognostic system that can monitor the state of health of the power modules in electric, hybrid, and fuel-cell vehicles. A special degradation trace on the V_{CEsat} of the insulated-gate bipolar-transistor modules was observed by a power-cycling accelerated test, which was not reported in literatures. A prognostic system based on utilizing the aforementioned trace is then developed. The system consists of the hardware architecture and current adaptive-algorithm-based software architecture. In addition, this prognostic system hardly increases the hardware cost on existing vehicle-driver system. An extensive simulation based on MATLAB/Simulink verifies the developed prognostic system.

Index Terms—Electric vehicles, electronics module, hybrid vehicles, reliability.

Fig. 1. Typical IGBT power module.

I. INTRODUCTION

HYBRID electric vehicles have recently achieved significant market penetration and stimulated a great amount of research work [1]–[3]. Cost-effective high-efficiency integrated power-electronic modules are one of the key elements toward making practical electric propulsions to control the electric-drive motors. The reliability of these power modules is of paramount impor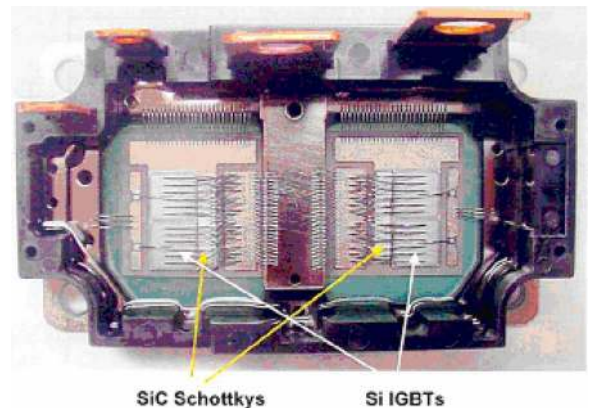tance for the commercial success of various types of electric vehicles. Electric-drive trains, due to their wide dynamic range of operation and diverse usage profiles, impose a stringent reliability requirement on the power modules than any other industrial motor-control applications.

As shown in Fig. 1, a typical power module has hundreds of wire bonds and numerous solder joints, which are subject to thermomechanical stress and fatigue caused by unavoidable power dissipation in the module. The reliability of power-semiconductor modules has been a concern for many industrial systems, particularly for the railway-traction applications in Europe and Japan, since their market introduction in early 1990s. Module failures are reported in literature both during power-cycling testing and in field usage [4]–[10]. Wire-bond lift-off and cracks at silicon-substrate or substrate-baseplate solder joints have been identified as the main failure mechanisms. Different operation conditions of the inverters result in varied inverter-phase current and power dissipation. This results in thermomechanical stress and fatigue. Power modules can and will fail, given enough stress and time. However, power modules usually go through a gradual degradation process before a catastrophic failure occurs. The degradation process shows some early symptoms on the state of health (SoH) of these power modules, including an increase in forward on-voltage, leakage current, thermal impedance, and, possibly, small signal impedance and noise level.
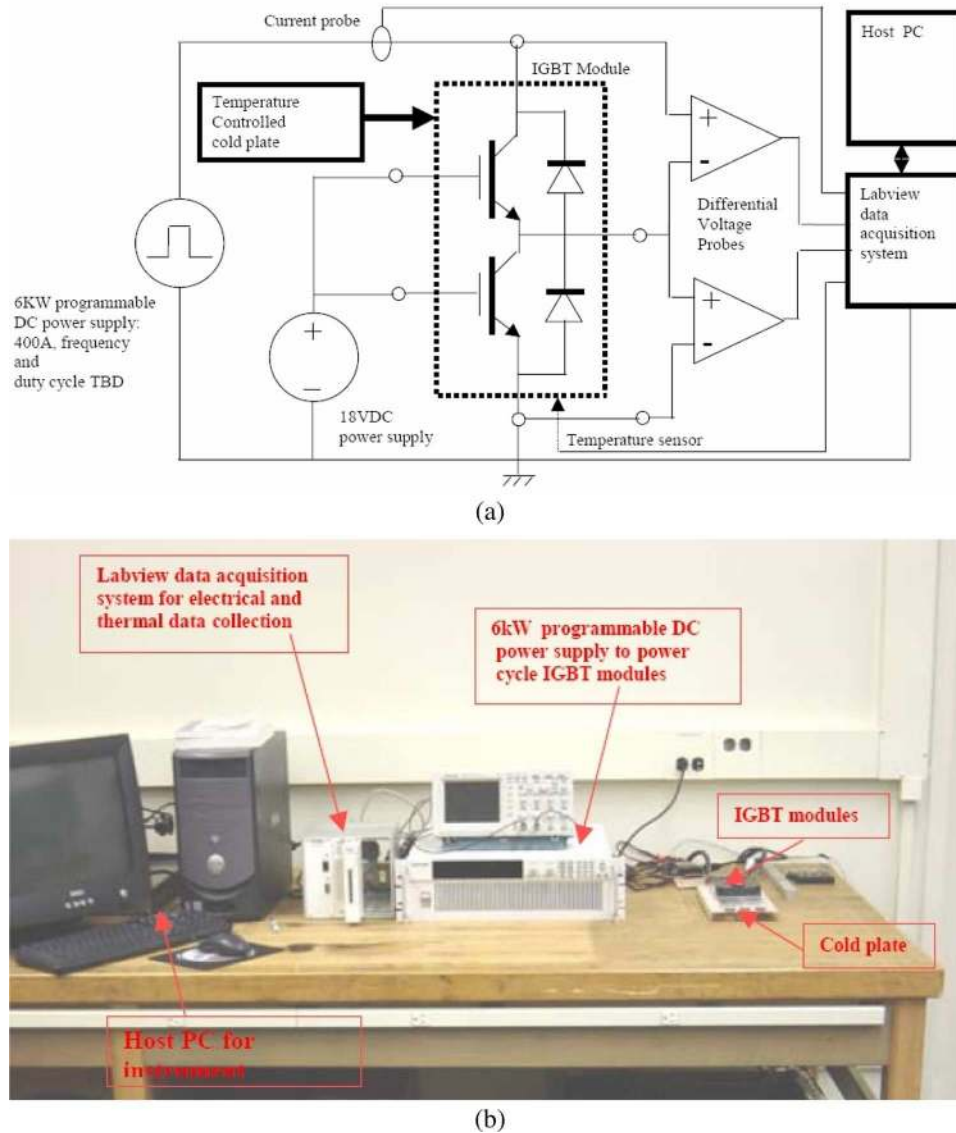
(a)

(b)

Fig. 2. Circuit diagram and system setup of the power-cycling accelerated stress test system for IGBT power modules.

The purpose of this paper is to develop an online diagnostic and prognostic system in electric, hybrid electric, and fuel-cell vehicles to warn the driver of potential failure of the power-electronic modules. Online diagnostics and condition monitoring were used in induction [11] and brushless dc motors [12], as well as internal combustion engines [13]. Yet, no work was reported to apply this approach in monitoring the SoH of power modules. In this paper, we first conducted a parametric investigation of power-module degradation processes. A computer-controlled stress test system was developed. Parametric measurement was taken periodically during the power-module stress testing. The measurement results were then analyzed to identify early warning signatures, which were used to provide onboard prognostic capability to monitor the SoH of power modules. Due to the complexity of deterioration mechanisms and the widespread parameter distribution of power modules, we have developed a practical algorithm to implement the prognostic function, to judge whether a
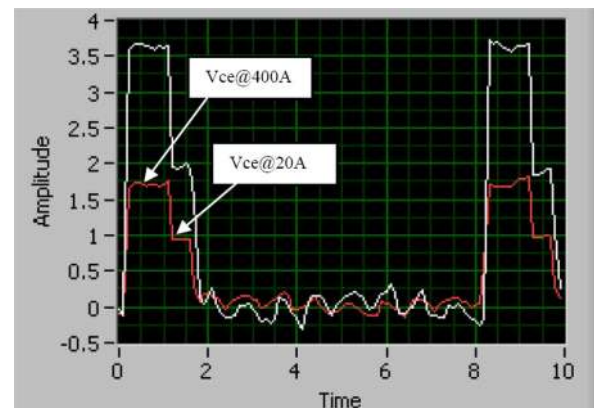

Fig. 3. V_{CEsat} waveforms of IGBT module under power-cycling test.

power module is on the verge of failing or in a good condition. The algorithm has been verified with extensive Simulink modeling.
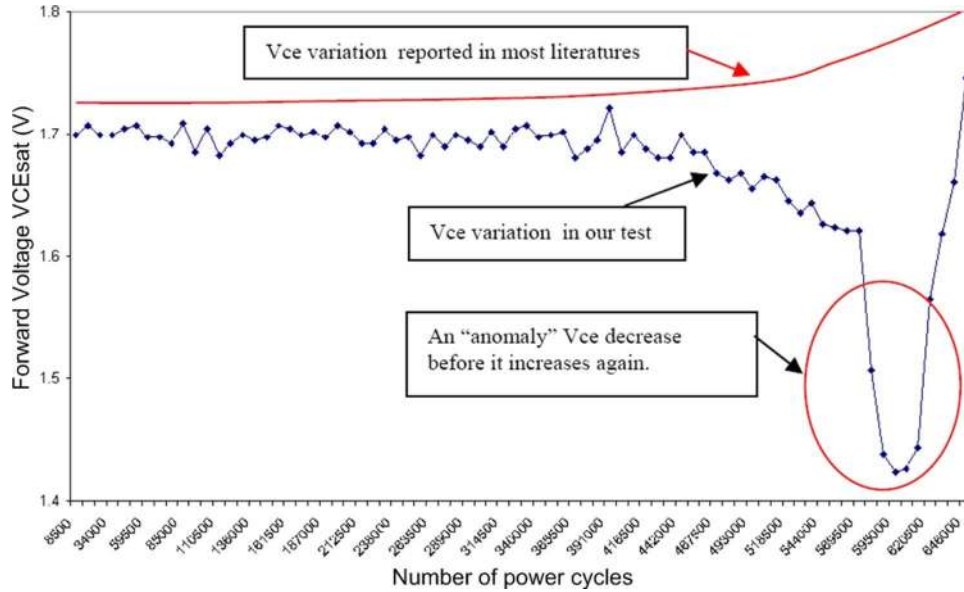
Fig. 4. V_{CEsat} at 400 A of IGBT module as a function of power cycles.

II. PARAMETRIC INVESTIGATION OF POWER-MODULE DEGRADATION

We have developed an accelerated stress-testing system to conduct a power-cycling test on power modules. The purpose of a power-cycling test is to emulate the operation of a power module in actual vehicles by subjecting the module to a series of power pulses. Our power-cycling test system consists of a 6-kW programmable dc power supply (Xantrex), a gate-drive circuit, a voltage sensor, a computer data-acquisition system (Labview), and a cold plate with water-circulation pump. The circuit diagram and system setup are shown in Fig. 2. A current pulse of 400 A with an on-time (heating) of 1 s and an off-time (cooling) of 9 s are used for the test. The case temperature is measured at about 65 °C and the internal junction temperature is extracted as 125 °C. The actual junction temperature of an insulated-gate bipolar transistor (IGBT) cannot be directly measured but is absolutely needed for setting up the duty cycle of power-cycling stress test and thermal-impedance characterization. Our solution is to measure a temperature-sensitive parameter of the IGBT to indirectly obtain the junction temperature. In this case, we used the collector-emitter saturation voltage (V_{CEsat}) of the IGBT as the temperature-sensitive parameter and established a lookup table of the V_{CEsat} as a function of ambient temperature to estimate the actual junction temperature of the IGBT. Since the testing was done at a low current in dc steady state in the environment chamber, the ambient temperature is approximately the same as the junction temperature.

The power-cycling test was implemented on a number of Toshiba MG800J2YS50A 600-V/800-A automotive IGBT power modules with a total logged testing time of approximately 10 000 h. The following are the test cycles: a 400-A current pulse with a duration of 1 s applied to the IGBTs, followed by a 20-A current pulse of 0.5 s and no current for 8.5 s before the cycle repeats itself. The forward voltage drop V_{CEsat} is constantly monitored by the data-acquisition system. The 400-A current pulse is estimated to raise the junction
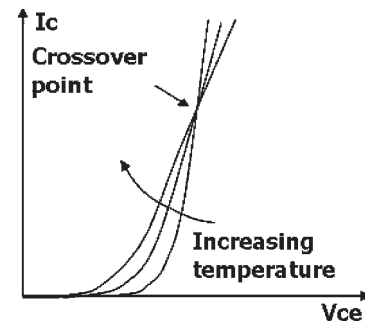

Fig. 5. I–V characteristics at different temperatures.

temperature by 55 °C. The 20-A current pulse provides a way of estimating actual junction temperature by comparing to the V_{CEsat} versus junction-temperature lookup table. Fig. 3 shows typical V_{CEsat} voltage waveforms of an IGBT module during the power-cycling test. The power-cycling data on the V_{CEsat} of the IGBT exhibits a significant degradation trace, as shown in Fig. 4. The V_{CEsat} of the IGBT remained unchanged until approximately 500 000 cycles. Then, it started decreasing gradually before a sudden drop (more than 17%) at around 600 000 cycles, followed by a quick increase in V_{CEsat}. At 648 000 cycles, V_{CEsat} exceeded its starting value and continued to increase. While it is well known that the V_{CEsat} of IGBT modules increases after certain power cycles due to wire-bond lifting, this unexpected "dip and rebound" phenomenon was not reported in the literature before.

We suspect that the physical mechanisms for this on-voltage "anomaly" can be attributed to sequential events of solder-joint degradation followed by wire-bond lift-off.

An IGBT has nonunitary temperature dependence with its V_{CEsat}, as shown in Fig. 5. V_{CEsat} shows a positive temperature coefficient above a crossover current but shows a negative temperature coefficient below it. This is due to two competing factors in the total V_{CEsat} of an IGBT: the P-N junction between the P+ substrate and N-epi layer and the MOS channel. While
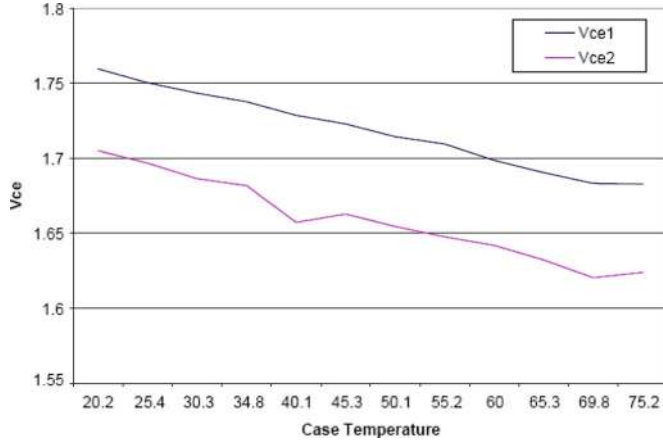
Fig. 6. V_{CEsat} at 400 A as a function of case temperature.

the V_{CEsat} contribution from the former factor decreases with increasing temperature, the later factor does the opposite due to the negative temperature dependence of electron mobility. For the IGBT modules under study, the measured V_{CEsat} at 400 A decreases with increasing junction temperature, as shown in Fig. 6. It is evident that V_{CEsat} decreases with increasing junction temperature, and 400 A is below the crossover point.

During the long power-cycling test process, the solder joints between the silicon chip and copper substrate degraded due to cracking or solder-void expansion, causing an increase in the thermal resistance of the whole module. This happened before the wire-bond lift-off failure occurred. When the testing conditions remained unchanged (same current pulse and case temperature), the junction temperature of the IGBT chip increased as a result of the higher thermal resistance. This, in turn, caused a decrease in the on-voltage of the IGBT module, as we have observed as an "anomaly." Eventually, the wire-bond lift-off failure occurred, causing a dramatic increase in the on-voltage, similar to all the reported data in the literature. This unique "signature" can be used to detect both solder-joint and wire-bond failures for the proposed prognostic algorithm development.

III. PARAMETRIC INVESTIGATION OF POWER-MODULE DEGRADATION

A quasi-real-time IGBT failure prognostic system has been developed to indicate the potential quilt-on-road risk. This algorithm is based on monitoring the abnormal V_{CEsat} variation at the specific current and temperature conditions. The basic idea is as follows: an IGBT will be considered as being seriously "degraded" if its measured V_{CEsat} deviates more than $\pm 15\%$ from its "normal" reference value. However, it is difficult to facilitate such a comparison considering the wide and fast variation of operating currents and temperatures of the IGBT module during actual vehicle operation. An adaptive approach is therefore developed to address this issue.

Currently, motor drives of electric power train are based on field-oriented control strategy. Where an ac motor is under variable-speed operation, the frequency and amplitude of its phase currents vary rapidly over a wide range, making the real-time and accurate detection and comparison of V_{CEsat} a
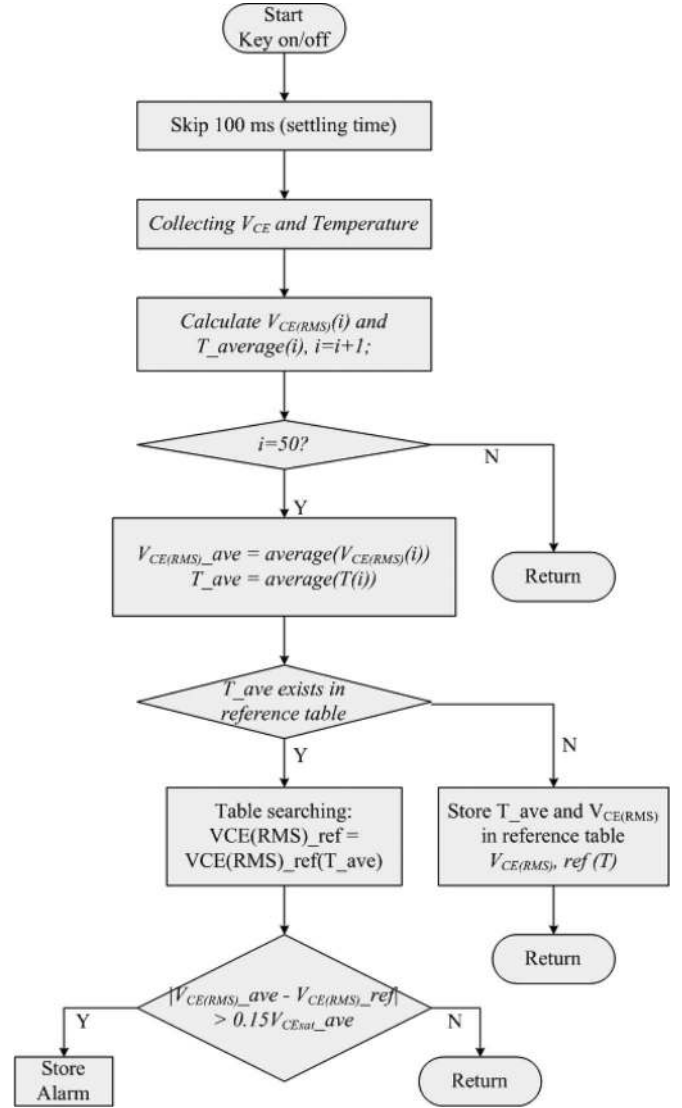

Fig. 7. Flowchart of the prognostic algorithm.

daunting challenge. A large 2-D reference lookup table (matrix) would be required to record the data for a wide range of currents and temperatures, resulting in an excessive memory requirement. Moreover, the "snap shot" nature of real-time V_{CEsat} data collection mandates an unreasonably high bandwidth of the data-sensing and A/D conversion circuitry. Fluctuations in measurement data could still easily exceed the $\pm 15\%$ comparison criteria.

In order to overcome these practical barriers, we have developed a strategy that inserts a prognostic subroutine to the vehicle control system immediately after the key-on and/or key-off of each vehicle-use period. The check-up routine typically lasts no more than a fraction of a second and does not change the normal operation of the vehicle. During the check-up period, the motor drive is forced to operate at a phase current with a preset frequency (e.g., 60 Hz) and amplitude (e.g., 200 A). We use the root-mean-square (rms) value of extracted V_{CEsat} to account for the average thermal effect. Comparing $V_{\text{CE(rms)}}$ at a fixed-frequency and fixed-amplitude sinusoidal phase current results in a significantly reduced size of the reference lookup table and measurement errors.
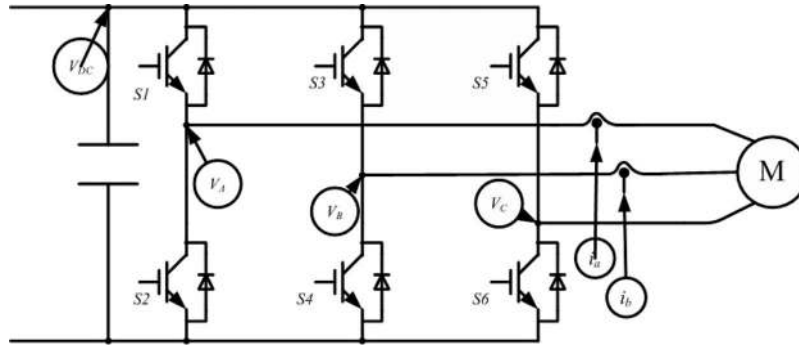
Fig. 8.   Power topology of three-phase VSI with voltage and current sensors.

Fig. 7 shows a simplified flowchart of the prognostic algorithm. Immediately after the key-on and/or key-off of each vehicle-use period, the prognostic algorithm is initiated. After the first 100 ms settling time, V_{CEsat} and module-temperature T data will be collected by voltage and temperature sensors. Due to the pulsewidth-modulation (PWM) frequency of the check up system that is designed as 5000 Hz, from the Shannon sample theory, the sampling rate of A/D is 100 000 Hz, which is a normal A/D speed for the current technology.

We calculate the rms value $V_{\text{CE(rms)}}(i)$ and average junction temperature $T\_average(i)$ using the collected V_{CEsat} data over full cycles of the phase current. We then take the average of 50 $V_{\text{CE(rms)}}(i)$ and $T\_average(i)$ data points to further minimize random data fluctuations. $V_{\text{CE(rms)}}(i)$ is calculated as the following:

$$V_{\text{CE(rms)}}(0)$$
$$= \sqrt{\frac{1}{n} \sum_{n=1}^{N} V_{\text{CE}}^2(n)} \tag{1}$$
$$V_{\text{CE(rms)}}(i)$$
$$= \sqrt{\frac{1}{N} \left(N \cdot V_{\text{CE(rms)}}^2(i-1) + V_{\text{CE}}^2(N+i) - V_{\text{CE}}^2(i) \right)} \tag{2}$$

where N is the number of sampling points per cycle of the sinusoidal phase current. It should be noted that, after the first $V_{\text{CE(rms)}}(0)$ is calculated, the next $V_{\text{CE(rms)}}(i)$ is calculated using only one additional sampling data point, which considerably reduces computation and memory requirements.

The same prognostic subroutine provides the following two basic functions: building an adaptive lookup table to provide a "nominal" reference value for $V_{\text{CE(rms)}}$ and comparing the collected $V_{\text{CE(rms)}}$ data to the reference value. When an average junction temperature T_ave is obtained, the subroutine will first search for the lookup table to see if a reference value already exists in the table. If not, the calculated $V_{\text{CE(rms)}}\_ave$ corresponding to the junction temperature of T_ave will be stored in the lookup table as a reference value $V_{\text{CE(rms)}}\_ref(T)$. Otherwise, the newly calculated $V_{\text{CE(rms)}}\_ave$ will be compared to the reference $V_{\text{CE(rms)}}\_ref$ at the same junction temperature T_ave. If the difference is greater than the $\pm15\%$ threshold, a warning signal will be sent out or stored in memory. Otherwise, the prognostic subroutine will exit.
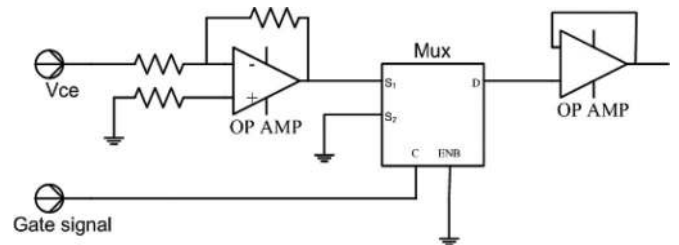

Fig. 9. V_{CE} OFF-state data-filter circuit diagram.

Assuming that a brand new IGBT module is in good condition, an assumption guarded by design and component incoming inspection, the prognostic algorithm will take days or even weeks to build up the reference lookup table, depending on how the brand new vehicle is used. It should be pointed out that some extremely low or high junction-temperature reference points in the table may never be established, depending on the usage environment of the vehicle (e.g., Arizona versus Alaska locations). Nevertheless, running the prognostic program at both the key-on and key-off of the vehicle can help in establishing the reference table over a large temperature range more quickly. For example, the junction temperature of the IGBT module at the key-off after a 2-h drive can be reasonably high even during winter months in Alaska. Similarly, the junction temperature at the key-on in the morning can be reasonably low even during summer months in Arizona. Most importantly, a warning signal will be generated by the prognostic algorithm if the difference between the measured and reference exceed the $\pm15\%$ threshold at any junction temperature. Despite diversified vehicle-usage patterns, the self-adaptive prognostic program can help capture the early warning symptoms of IGBT-module degradation.

IV. PROGNOSTIC-SYSTEM HARDWARE IMPLEMENTATION

Ideally, the prognostic system can be implemented within the existing vehicular hardware and software architecture. A typical ac-drive system already has the following sensors: one bus-voltage sensor V_{DC} and two phase-current sensors I_{a} and I_{b}. In addition, it may have some temperature sensors embedded in the IGBT power modules. All these existing current, voltage, and temperature sensors will be used to implement the prognostics system. In addition, three extra voltage sensors are placed at the positions a, b, and c, as shown in Fig. 8. They can directly obtain the V_{CE} on three bottom-leg IGBT chips, V_a, V_b, and V_c.
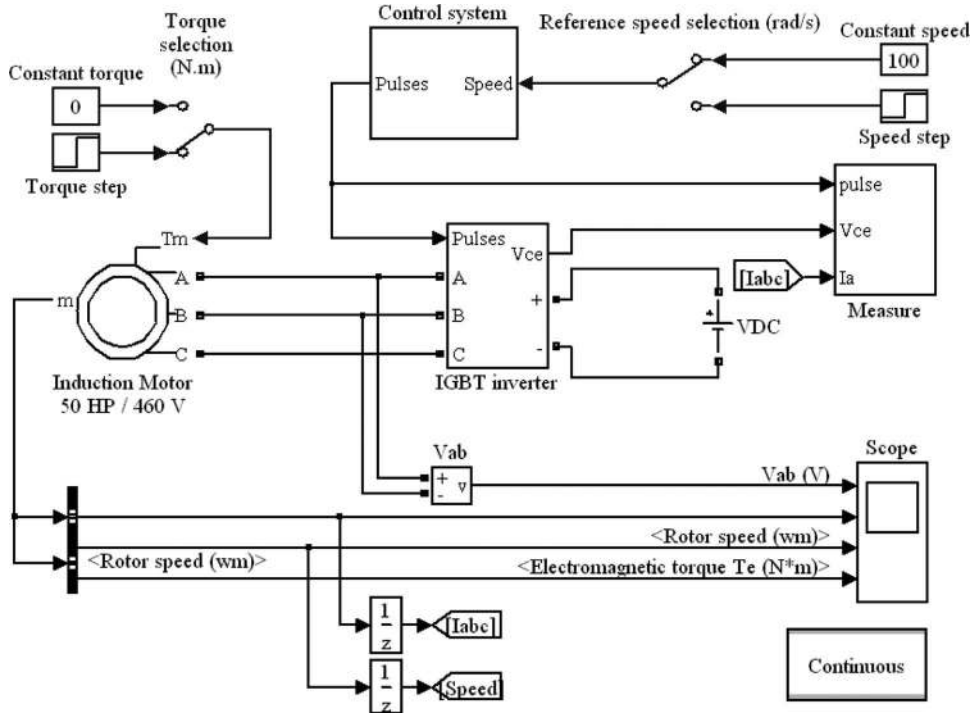
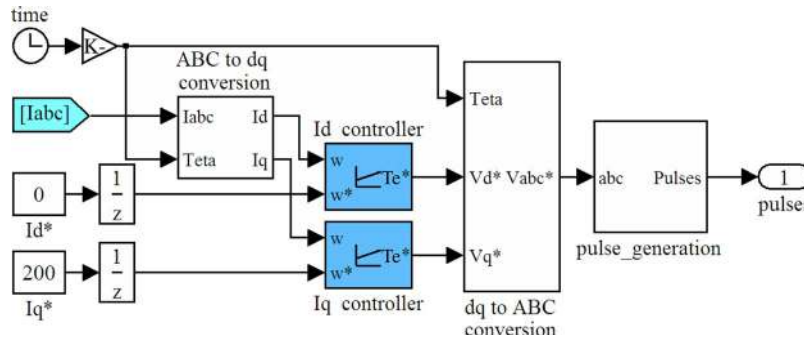Fig. 10. Simulink block diagram of the prognostic system.

Fig. 11. Control block of the IGBT-module diagnostic-control mode.

The $V_{\rm CE}$ on three upper leg IGBT chips can be obtained from $V_{\rm DC}$ and V_a, V_b, and V_c, respectively.

The major challenge in sensing $V_{\rm CE}$ is that the IGBT has a much lower $V_{\rm CE}$ value in the ON-state (typically, 1.5–2.5 V) than that of the OFF-state (typically, 200–400 V). Since the purpose of our prognostic algorithm is to monitor $V_{\rm CEsat}$, we need to filter out the OFF-state $V_{\rm CE}$ data to avoid measurement errors.

A two-to-one multiplexer circuit is used to filter out the OFF-state data, as shown in Fig. 9. The gate-drive signal of the IGBT is utilized to select one of the multiplexer's inputs as its output. The scaled detected $V_{\rm CE}$ is one of the inputs $S1$ of the multiplexer, and ground (zero) is the other input signal $S2$. When the gate signal is "1," which means that the IGBT is switched on, the detected $V_{\rm CE}$ signal $V_{\rm CEsat}$ is the output signal. When the gate signal is "0," the IGBT is switched off. Zero is now the output signal. In practice, the switching delay of an IGBT should be considered.

V. SIMULINK-MODELING VERIFICATION

An extensive MATLAB/Simulink simulation was performed to verify the prognostic system. Fig. 10 shows the schematic of the hybrid ac-drive and IGBT failure prognostic system. First, we simplify the model of a vehicle's drive system as an ac-drive system. As a regular ac drive used in vehicles, a voltage-source inverter (VSI) provides controllable power for an induction motor to regulate the electromagnetic torque of the motor and then control speed of the motor. Here, a prognostic control block is added to the conventional motor-drive system to provide prognostic functions at the key-on and/or key-off of the vehicle.

When the vehicle is starting up and/or turning off, the prognostic control block substitutes the ac-drive control strategy. The control block is shown in Fig. 11. Its control objective is to generate the phase current of the system with fixed frequency and amplitude.

The control method, which imitates the vector control of motors, is established in this simulation. The reference currents are given in the synchronously rotating frame as I_d^* and I_q^* commands. Time index t is used to be the angular-position reference at synchronously rotating frame. $2\pi f \cdot t$ is then used as θ at ABC-coordinate to $d-q$ coordinate conversion, where f is frequency of phase currents. The detected phase currents are converted into the synchronously rotating frame as I_d and I_q. Then, actual I_d/I_q and their reference I_d^*/I_q^* are used to generate V_d^* and V_q^* commands through the proportional–integral (PI) compensators, as shown in Fig. 11. These voltage commands are then converted into stationary-frame instantaneous-phase voltages, which are the modulation signals to be compared with triangular signal to obtain IGBTs' gate-drive signals. Controlling IGBT gate signals makes currents flow through the IGBT inverter track the reference current I_d^* and I_q^* commands. Because of the sluggish response of the induction motor, when the system is conducting the prognostic process, the parameters of the motor are nearly constant. This makes it easy to set up the parameters of the PI compensators.

When the control strategy works effectively to produce the required phase currents, the prognostic algorithm, as shown in Fig. 7, can probe the SoH of the IGBT module. Other main simulation conditions are as follows.

1) The R_{dson} of one IGBT chip is purposely reduced to half of its normal value at 73 ms and, then, restored to its normal value at 150 ms in this simulation. This R_{dson} change simulates the IGBT-degradation process.
2) The motor is rated as 50 hp and 460-V line voltages.
3) The phase current at prognostic status has 60-Hz frequency and 200-A amplitude.

The simulation results are shown in Fig. 12(a)–(e). It should be noted that the rms calculation algorithm is designed to calculate the rms value of the 60-Hz fundamental frequency signal. The rms value for the signal with frequency other than 60 Hz is meaningless.

Fig. 12(a) is the phase-current waveform. We can find that the control strategy is proved to be effective to make sure the phase current is of 60-Hz frequency and 200-A amplitude. After 300 mS, control system is changed to speed-control strategy. The phase current is modulated to control the torque of motor. Fig. 12(b) and (d) is the waveform of the extracted i_{DS} and V_{CEsat} with the method aforementioned, respectively. The PWM-like waveform can be easily observed from these figures. Fig. 12(c) and (e) is the 60-Hz-based rms value corresponding to Fig. 12(b) and (d), respectively. We can see that we have one cycle delay at the rms-value calculation. For the prognostic system, the delay is acceptable. When the IGBT chip degrades at 73 ms, the $V_{\mathrm{CE(rms)}}$ value has a significant change correspondingly. This symptom is captured by the diagnostic algorithm to produce the warning signal.

VI. Summary

In summary, we have conducted parametric study of IGBT power-module degradation under power-cycling conditions. The power-cycling accelerated test has revealed a signature degradation trace on the V_{CEsat} of the IGBT modules, which
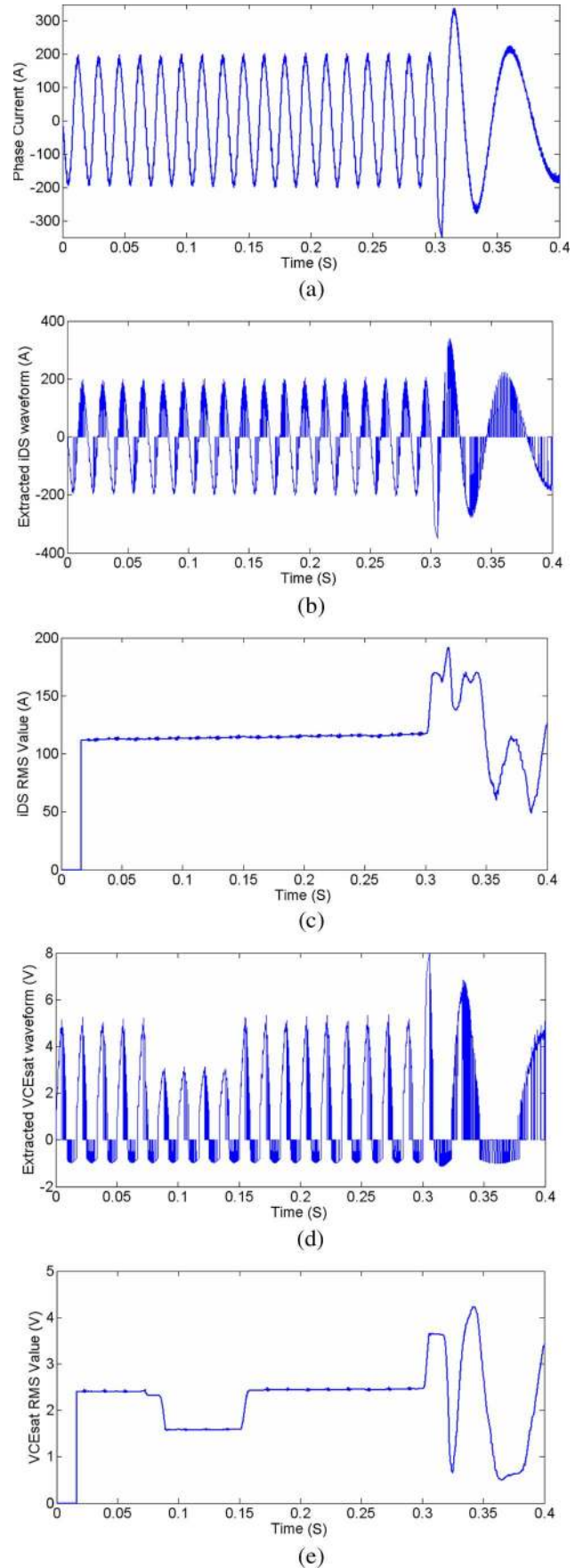

Fig. 12. Simulation results (a) phase current. (b) Extracted i_{DS}. (c) RMS value of (b). (d) Extracted V_{CEsat}. (e) RMS value of (d).

was not reported in literatures. The signature degradation trace is used to develop the prognostic system for IGBT modules to detect the following two major failure mechanisms: the solder-joint degradation and wire-bond lift-off.

Based on the trace we have observed, we have developed a prognostic system that can monitor the SoH of the power modules in electric, hybrid, and fuel-cell vehicles. This paper presents the detailed realization of the prognostic system, which consists of the hardware architecture and current adaptive-algorithm-based software architecture. The designed prognostic system hardly increases the hardware cost of the existing vehicle-drive system. A computer simulation based on MATLAB/Simulink verifies the developed prognostic system.

REFERENCES

[1] J. Moreno, M. E. Ortuzar, and J. W. Dixon, "Energy-management system for a hybrid electric vehicle, using ultracapacitors and neural networks," *IEEE Trans. Ind. Electron.*, vol. 53, no. 2, pp. 614–623, Apr. 2006.

[2] H.-D. Lee and S.-K. Sul, "Fuzzy-logic-based torque control strategy for parallel-type hybrid electric vehicle," *IEEE Trans. Ind. Electron.*, vol. 45, no. 4, pp. 625–632, Aug. 1998.

[3] M. Ehsani, K. M. Rahman, M. D. Bellar, and A. J. Severinsky, "Evaluation of soft switching for EV and HEV motor drives," *IEEE Trans. Ind. Electron.*, vol. 48, no. 1, pp. 82–90, Feb. 2001.

[4] J. Onuki, M. Koizumi, and M. Suwa, "Reliability of thick Al wire bonds in IGBT modules for traction motor drives," *IEEE Trans. Adv. Packag.*, vol. 23, no. 1, pp. 108–112, Feb. 2000.

[5] W. Wu, M. Held, P. Jacob, P. Scacco, and A. Birolini, "Investigation on the long term reliability of power IGBT modules," in *Proc. 7th ISPSD ICs*, May 23–25, 1995, pp. 443–448.

[6] P. Jacob, M. Held, P. Scacco, and W. Wuchen, "Reliability testing and analysis of IGBT power semiconductor modules," in *Proc. IEE Colloq. IGBT Propulsion Drives*, Apr. 25, 1995, pp. 4/1–4/5.

[7] V. Mehrotra, J. He, M. S. Dadkhah, K. Rugg, and M. C. Shaw, "Wire-bond reliability in IGBT-power modules: Application of high resolution strain and temperature mapping," in *Proc. ISPSD ICs*, May 26–28, 1999, pp. 113–116.

[8] A. Hamidi, S. Kaufmann, and E. Herr, "Increased lifetime of wire bonding connections for IGBT power modules," in *Proc. APEC*, Mar. 4–8, 2001, vol. 2, pp. 1040–1044.

[9] Y. Nishimura, K. Oonishi, A. Morozumi, E. Mochizuki, and Y. Takahashi, "All lead free IGBT module with excellent reliability," in *Proc. ISPSD ICs*, May 23–26, 2005, pp. 79–82.

[10] A. Morozumi, K. Yamada, T. Miyasaka, S. Sumi, and Y. Seki, "Reliability of power cycling for IGBT power semiconductor modules," *IEEE Trans. Ind. Appl.*, vol. 39, no. 3, pp. 665–671, May/Jun. 2003.

[11] J. F. Martins, V. F. Pires, and A. J. Pires, "Unsupervised neural-network-based algorithm for an on-line diagnosis of three-phase induction motor stator fault," *IEEE Trans. Ind. Electron.*, vol. 54, no. 1, pp. 259–264, Feb. 2007.

[12] S. Rajagopalan, J. M. Aller, J. A. Restrepo, T. G. Habetler, and R. G. Harley, "Analytic-wavelet-ridge-based detection of dynamic eccentricity in brushless direct current (BLDC) motors functioning under dynamic operating conditions," *IEEE Trans. Ind. Electron.*, vol. 54, no. 3, pp. 1410–1419, Jun. 2007.

[13] G. F. Mauer, "On-line cylinder fault diagnostics for internal combustion engines," *IEEE Trans. Ind. Electron.*, vol. 37, no. 3, pp. 221–226, Jun. 1990.

Yali Xiong (S'07) received the B.S.E.E. and M.S.E.E. degrees from the Huazhong University of Science and Technology (HUST), Wuhan, China, in 1998 and 2001, respectively. She is currently working toward the Ph.D. degree in the School of Electrical Engineering and Computer Science, University of Central Florida, Orlando.

She was a Faculty Member with the Electrical Engineering and Computer Science Department, HUST. Her research interests include power electronics and power semiconductors.

Xu Cheng (M'99) received the B.S. degree in solid-state electronics from the Huazhong University of Science and Technology, Wuhan, China, in 1992 and the M.S. and Ph.D. degrees in microelectronics from the Beijing University of Technology (BUT), Beijing, China, in 1995 and 2004, respectively.

He was an Associate Professor of electrical engineering with BUT. He held a visiting position with the Department of Electrical and Computer Engineering, University of Central Florida, Orlando. He is currently with Freescale Semiconductor, Inc., Tempe, AZ. His research interests include design, modeling, and characterization of power-semiconductor devices and integrated circuits. He has more than 15 publications in these research areas.

Z. John Shen (S'90–M'04–SM'02) received the B.S. degree in electrical engineering from Tsinghua University, Beijing, China, in 1987 and the M.S. and Ph.D. degrees in electrical engineering from Rensselaer Polytechnic Institute, Troy, NY, in 1991 and 1994, respectively.

From 1994 to 1999, he held a number of technical positions, including as a Senior Principal Staff Scientist with Motorola Semiconductor Products Sector, Phoenix, AZ. From 1999 to 2004, he was with the University of Michigan, Dearborn. In 2004, he joined with the School of Electrical Engineering and Computer Science, University of Central Florida, Orlando, where he is currently an Associate Professor of electrical engineering, a Director with the Power Semiconductor Research Laboratory, and an Associate Director with the Florida Power Electronics Center. He has more than 80 journal and referred conference publications in these areas. He is also the holder of nine issued and numerous pending U.S. patents in these areas. He is the inventor of the world's first sub-miliohm power MOSFET. His current research interests include power semiconductor devices and integrated circuits, power electronics, automotive electronics, nanotechnology, and renewable-energy systems.

Prof. Shen currently serves as an at-large AdCom member of the IEEE Power Electronics Society. He is currently an Associate Editor for the IEEE TRANSACTIONS IN POWER ELECTRONICS. He also served as the Technical Program Chair of the 38th IEEE Power Electronics Specialists Conference in 2007 and the First IEEE Vehicle Power and Propulsion Conference in 2005. He also served on the organizing committees of several other IEEE conferences and workshops. He was the recipient of the 2003 U.S. National Science Foundation CAREER Award, the 2006 Transaction Prize Paper Award of the IEEE TRANSACTION ON POWER ELECTRONICS from the IEEE Power Electronics Society, the 2003 IEEE Best Automotive Electronics Paper Award from the IEEE Vehicular Technology Society, and the 1996 Motorola Science and Technology Award.

Chunting Mi (S'00–A'01–M'01–SM'03) received the B.S.E.E. and M.S.E.E. degrees in electrical engineering from Northwestern Polytechnical University, Xi'an, China, and the Ph.D. degree in electrical engineering from the University of Toronto, Toronto, ON, Canada.

From 1988 to 1994, he was with the Rare-Earth Permanent Magnet Machine Institute, Northwestern Polytechnical University. In 1994, he was with Xi'an Petroleum Institute, Xi'an, as an Associate Professor and Associate Chair of the Department of Automation. From 1996 to 1997, he was a Visiting Scientist with the University of Toronto. In 2000, he was an Electrical Engineer with General Electric Canada Inc., Peterborough, ON, where he was responsible for designing and developing large electric motors and generators. He is currently an Associate Professor with the Department of Electrical and Computer Engineering, University of Michigan, Dearborn, and a Director with the newly developed Directorate of Technical Education Power Electronics Laboratory. His teaching and research interests include power electronics, hybrid electric vehicles, electric machines and drives, renewable energy, and control.

Prof. Mi is the Vice Chair and Chair-Elect of the IEEE Southeastern Michigan Section. He was the recipient of many technical awards, including the Government Special Allowance (China), the Technical Innovation Award (China), the Distinguished Teaching Award from the University of Michigan, the 2007 IEEE Region 4 "Outstanding Engineer Award," the 2007 IEEE Southeastern Michigan Section "Outstanding Professional Award," and the 2007 SAE Environmental Excellence in Transportation (E2T) Award.

Hongjie Wu received the M.S. degree in electrical engineering from the China University of Mining Technology, Beijing, China, in 2000 and the M.S. degree in electrical engineering from the University of Michigan, Dearborn, in 2006.

In 2000, he was with Bell Labs, Lucent Technologies, where he worked on the communication-power system research and development. Since 2006, he has been with Ford Motor Company, Dearborn, where he is currently working on the HEV E-Drive system research and development.

Vijay K. Garg (S'71–M'75–SM'79–F'95) received the B.S.E.E. degree from Roorkee University, Roorkee, India, in 1962 and the M.S. and Ph.D. degrees in electrical engineering from Virginia Polytechnic and State University, Blacksburg, in 1972 and 1975, respectively.

He was a Senior Technical Specialist with the Ford Research Center, Ford Motor Company, Dearborn, MI, from 1995 to 2007 and a Fellow Engineer with the Westinghouse Research Center. He is currently with Caterpillar Inc., Peoria, IL. His interests include automotive electric-drive systems, electromagnetics (EM), and EM devices. He is the author or a coauthor of more than 45 technical papers in various international journals and conference proceedings. He is the holder of 15 U.S. patents.

Dr. Garg was the Chair of the Electrical and Electronics Technical Committee of FreedomCAR (a U.S. Department of Energy Consortium) from 2004 to 2007.